doi:10.1017/S1431927620020632
Microsc. Microanal. 26 (Suppl 2), 2020

Characterization of Combustion Synthesis of Ferromagnetic $FeAl_2O_4$ spinel

Renan Loreto[1], Jesana Silva[2], Jefferson Araujo[2] and Guillermo Solórzano[2]

[1]CBPF, Rio de Janeiro, Rio de Janeiro, Brazil, [2]PUC-Rio, Rio de Janeiro, Rio de Janeiro, Brazil

In recent years, there is increasing interesting in multifunctional ceramic materials, arising from both intriguing fundamental properties and potential applications. Spinel with general formula AB_2O_4 and FCC structure is typical of such interest [1-2]. Several synthesis methods for these materials have been proposed, including co-precipitation, sol-gel [3], and combustion reaction synthesis [4]. The last is particularly convenient because of its low costs, high-reaction speed, and also energy efficient as the reaction release energy, which is contrary to other techniques mentioned [5]. In this work we synthetize and characterize $FeAl_2O_4$ spinel because of its magnetic properties and wide possibility of applications. The combustion reaction method for obtaining $FeAl_2O_4$ has been used starting with a solution of hydrated iron and aluminum nitrites (molar ratio 1:2) and citric acid as combustion source and varying the stoichiometry of the latter. Such solutions were mixed and heated up to 500 °C in a hot plate until ignition occurred, burning and the production of a solid products in a powder form [6]. This method is particularly advantageous compared to other combustion synthesis since does not require a muffle furnace, complex combustibles [4] or multiple combustibles [5]. The final product has been characterized in terms of structure and compositional by means of X-ray diffraction (DRX - Panalytical), and Analytical Electron Microscopy (AEM): scanning electron microscopy (SEM JEOL 7100F) and scanning and transmission electron microscopy (TEM/STEM – JEOL 2100F), aiming at phase identification of the solid product as well as detailed morphological characterization. Magnetic properties were obtained by vibrating sample magnetometry (VSM) at room temperature. Figure 1 shows the diffractograms for three samples, according to the stoichiometry of the combustible [6], in ideal concentration (sample AFA, in green), 10% below ideal (sample AFA-, in orange) and 10% above ideal (sample AFA+, in maroon). In this case we can see the results corresponds to a multiphasic material with typical structure of $FeAl_2O_4$, spinel (JCPDF 01-089-1685) and hematite (JCPDF 00-013-0534) as a second phase material. Figures 1b, 1c and 1d are secondary-electrons (SE) and Figures 1e, 1f and 1g backscattered electron (BSE) SEM images where both SE and BSE signals shows the solid agglomerated products as multiphase material with a granular morphology and grains size in the order of 40 to 50 nm. Figure 2a, 2b and 2c are bright field (BF) TEM image for AFA, AFA- and AFA+ respectively. Figures 2d, 2e and 2f are dark field (DF) images with the corresponding diffraction patterns of AFA, AFA- and AFA+ samples respectively. TEM confirms the nature of crystalline aggregates with particle size as before mentioned in the order 40-50 nm. TEM images also reveals the same morphological and particle size distribution for all synthesis conditions. The magnetic hysteresis (M x H) curves of samples AFA, AFA- and AFA+, with a typical behavior of a ferromagnetic material but with narrow curves, characteristic of a soft magnetic material ($H_c \approx 47$ Oe for sample AFA) and low remanent magnetization ($M_r \approx 0{,}72$ emu/g for sample AFA). In summary, the combustion synthesis with only citric acid as a combustible have synthetized the $FeAl_2O_4$ spinel, among other phases as hematite. Further studies with other combustibles, such as urea, might be more efficient in the formation of pure phase iron-aluminate spinel.

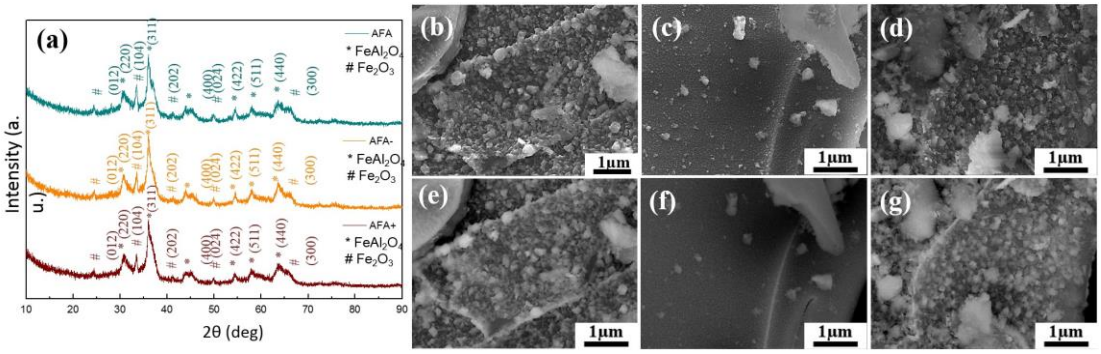

Figure 1. (a) X-ray diffractogram of sample AFA, AFA- and AFA+; (b) (c) (d) SE and (e) (f) (g) BSE SEM image of samples AFA, AFA- and AFA+, respectively.

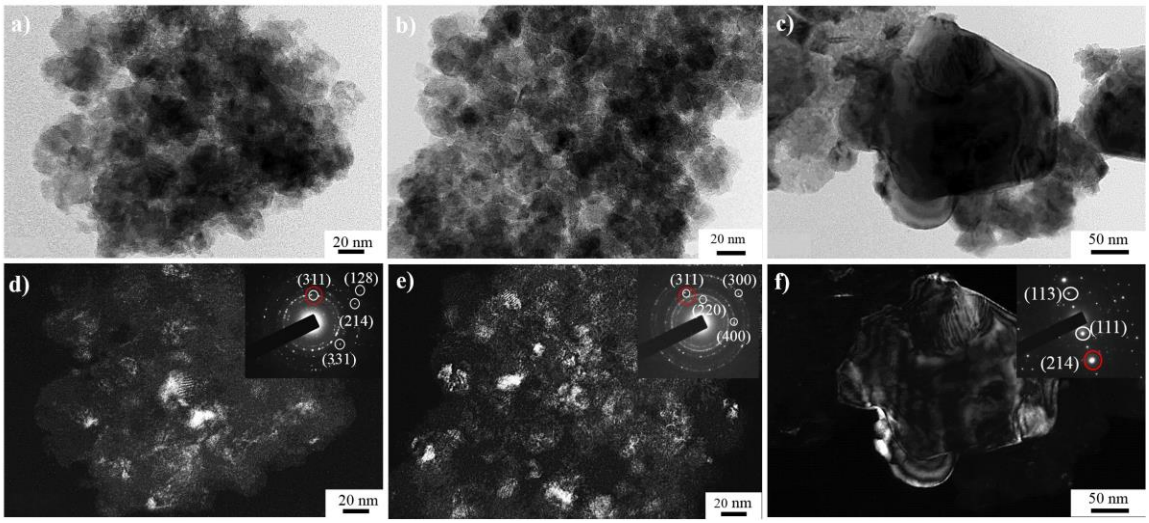

Figure 2. (a), (b) and (c) BF-TEM image of samples AFA, AFA- and AFA+, respectively; (d), (e) and (f) DF-TEM images of samples AFA, AFA- and AFA+, respectively, and corresponding diffraction pattern.

References

[1] J. Ilona, et al. EUR J MINERAL. 29, (2017) 63–72.
[2] D.P. Dutta, et al. Materials Science and Engineering B 176, (2011) 177–180.
[3] M. Azam et al. Materials Today: Proceedings 2, (2015) 5150 – 5154.
[4] S. Maiti et al. Journal of Power Sources 304, (2016) 319-331.
[5] M. Chai et al. Chemistry Letters 43 (2014), 1743-1745.
[6] L. Durães et al. Journal of the European Ceramic Society 32 (2012) 3161–3170

https://doi.org/10.1017/S1431927620020632 Published online by Cambridge University Press